PNAS
www.pnas.org

SUPPLEMENTARY INFORMATION

Polar In-Plane Surface Orientation of a Ferroelectric Nematic Liquid Crystal: Polar Monodomains and Twisted State Electro-Optics

Xi Chen[a,b], Eva Korblova[b,c], Matthew A. Glaser[a,b], Joseph E. Maclennan[a,b], David M. Walba[b,c], Noel A. Clark[a,b]*

[a]*Department of Physics, University of Colorado, Boulder, CO 80309, USA*

[b]*Soft Materials Research Center, University of Colorado, Boulder, CO 80309, USA*

[c]*Department of Chemistry, University of Colorado, Boulder, CO 80309, USA*

**Corresponding Author* - Noel Clark (*noel.clark@colorado.edu*)

Abstract

We show that surface interactions can vectorially structure the three-dimensional polarization field of a ferroelectric fluid. The contact between a ferroelectric nematic liquid crystal and a surface with in-plane polarity generates a preferred in-plane orientation of the polarization field at that interface. This is a route to the formation of fluid or glassy monodomains of high polarization without the need for electric field poling. For example, unidirectional buffing of polyimide films on planar surfaces to give quadrupolar in-plane anisotropy also induces macroscopic in-plane polar order at the surfaces, enabling the formation of a variety of azimuthal polar director structures in the cell interior, including uniform and twisted states. In a π-twist cell, obtained with antiparallel, unidirectional buffing on opposing surfaces, we demonstrate three distinct modes of ferroelectric nematic electro-optic response: intrinsic, viscosity-limited, field-induced molecular reorientation; field-induced motion of domain walls separating twisted states of opposite chirality; and propagation of polarization reorientation solitons from the cell plates to the cell center upon field reversal. Chirally doped ferroelectric nematics in antiparallel-rubbed cells produce Grandjean textures of helical twist that can be unwound via field-induced polar surface reorientation transitions. Fields required are in the 3 V/mm range, indicating an in-plane polar anchoring energy of $w_P \sim 3\text{x}10^{-3}$ J/m^2.

TABLE OF CONTENTS

SECTION 1 *– CHIRAL DOPING OF THE FERROELECTRIC NEMATIC*

We have demonstrated that it is possible to manipulate N_F twisted states by chiral doping. To this end, we carried out electro-optic experiments on a chiral ferroelectric nematic (N_F*) phase, a mixture of RM734 with the widely-used chiral dopant CB15* [1,2,3] at a concentration c = 10 wt%. RM734 and CB15* mix in the I and N phases, but submicron-scale spots appear at the N to N_F transition, indicating that CB15* may phase separate to some extent. Given the inverse helical twisting power h^{-1} ~ 5 to 6 (μm wt%) of CB15* in standard nematic hosts [1,2], we would expect the chiral nematic pitch at a concentration c wt% to be in the range 1.6 μm < $p \sim 1/hc <$ 2.0 μm. In the experiments reported below, we estimate the pitch in the N_F phase to be p ~ 2.3 μm, at the high end of the expected range.

The chiral mixture was filled into d = 3.5 μm thick *ANTIPOLAR* cells and subjected to in-plane fields in the range $0 < E < 8$ V/mm. The textures and corresponding cell structures observed in DTLM are shown in ***Fig. S1 .*** We observe a field-induced helix unwinding, mediated for positive ***E*** by surface transitions between preferred and metastable surface states (***Fig. 1B***), and for negative ***E*** by the bulk 2π twist disclinations of ***Fig 2***. The cell geometry is that of ***Fig. 2C***, so that, as discussed above, if E is nonzero the cell structure without liquid crystal is chiral, and changes handedness if the sign of ***E*** changes. Therefore, since the RM734/CB15* mixture is chiral and of fixed handedness, its response to positive and negative fields should be different, as is clearly observed in the experiments.

Positive Field Response – Optical changes are observed in an increasing positive E field, starting at E ~ 0.04 V/mm as seen in ***Fig. S1***. As the applied field is increased, we observe the sequential appearance of three topologically distinct states, the grey-to-yellow *initial* (*i*) state, the intermediate orange states (*b*,*t*), and the maroon-blue final, high-field state for positive E (*f+*), evidenced by the passage of sharp domain walls, as shown in ***Fig. S1A-E***. This observed sequence is interpreted under the assumption that, due to polarization charge stabilization, ***P*** in the bulk is everywhere in the *yz*-plane, as in the preceding discussions. The final (maroon *f+*) state achieved in this sequence evolves for yet higher field continuously from the maroon hue of ***Fig. S1E*** to the simulated blue color of ***Fig. 4K***. The continuous maroon-to-blue change indicates the absence of further surface transitions, and, instead, a field-induced distortion of the *f+* state, ending with a uniform orientation in the cell interior with a π/2 twist near each cell surface, as in ***Figs. S1K, 4D***, which can be considered the *final* high-field state. This state is held in by the field, which is necessary to maintain its surface orienttions in their metastable quadrupolar energy minima.

The $E = 0$ *initial* (*i*) state has the lowest effective birefringence of the sequence, implying that it is the most twisted (by some multiple of π because of the *ANTIPOLAR* surfaces), meaning that this

sequence of states corresponds to a field-induced unwinding of the director twist, as might be expected. A key feature of this sequence is that there are two distinct orange states, (*b* - *bottom*) and (*t* - *top*), that evolve from the *initial* state *i* via domain wall-mediated transitions. The *b* and *t* states have identical color and have the property that if pairs of *bb* or *tt* states come together, they can merge with no trace of a boundary. In contrast, *bt* domain pairs appear to overlap kaleidoscope-like to give the *final* state ($bt \rightarrow f+$), without physical interaction, but becoming a maroon color in the overlap region. Since the maroon *final* state is uniform (apart from a $\pi/2$ twist near each surface), the *i* to *b* and *t* and then to *f+* transformations must be topological transitions representing distinct but structurally equivalent expulsions of twist from the *i* state. These expulsions, when overlapped, give the *f+* state. Furthermore, because the *b,t* states have the same color, the cell must otherwise be uniform, meaning that if we let *i, b, t* ,and *f+* represent the net twist $\Delta\varphi$ in each state, we must have $i - b - t = f+$, or $i = 2b + \pi$, which, if we take $b,t = \pi$, the minimal angular jump for a topological transition in an *ANTIPOLAR* cell, gives $i = 3\pi$. The sequence $i \rightarrow b$ *or* $t \rightarrow f+$ is then a sequence of states where the net azimuthal change $\Delta\varphi$ between the two surfaces evolves with increasing *E* field as $3\pi \rightarrow 2\pi \rightarrow \pi$, with an $E = 0$ chiral pitch in the *initial* 3πT state of $p = 2.3\ \mu$m ($2d/3$). This value should be the bulk pitch, within a $\pm\pi/2$ reorientation at one surface. The polar director states corresponding to this sequence and the transitions between them are illustrated in Fig. ***S1F-J***. Of note is that the reductions in $\Delta\varphi$ at the $i \rightarrow b$ (or $i \rightarrow t$) events are mediated by *surface* orientational transitions from the global minimum in $W(\varphi)$ (the preferred surface polarization orientation) to the metastable minimum in $W(\varphi)$, sketched in the inset of ***Fig. 1B***.

DTLM images of the $\Delta\varphi = 3\pi$ *initial* state obtained with polarizer and analyzer uncrossed in opposite directions and compared with simulated spectral colors, as in ***Figs. 4I-K*** confirm that CB15* in the RM734 N* and N_F* phases is a right-handed nematic dopant, inducing a right-handed helix as it does in 5CB.

Negative Field Response – For negative *E*, the principal transition out of the *initial* 3πT state is to the field-induced *f-* state shown in ***Fig. S1Q***. This sign of field expands the partially aligned π-twist regions near the surfaces, leaving the surface orientations unchanged, and squeezing the central 2π twist into a thin metastable sheet, which is then eliminated by the heterogeneous nucleation of holes (2π dislocation loops) that spread and eventually fill the central plane, leaving the *f-* state. In the *f-* state, the field enforces uniform orientation in the cell interior, there are $\pi/2$ twist walls near each cell surface, and the surfaces remain at their preferred orientations. Note that this is structurally equivalent to the *f+* state but rotated by π, so that the two surfaces are in their preferred polar, rather than metastable quadrupolar, states, making the *f-* state the lowest energy field-induced state in the chirally doped cell. Both the *f+* and *f-* states are stabilized by the field, but they, and the *b,t* states, all relax in distinctly different ways when the field is re-

duced or removed. If the field is removed from the *f-* state, the director field finds itself extremely dilated relative to the *initial* $\Delta\varphi = 3\pi$ state, and return to the *i* state by the nucleation and passage of 2π bulk twist disclination, like that shown in ***Fig. 2E.***

Relaxation on Field Reduction –The behavior observed upon reducing the *positive* field back to $E = 0$ is sketched in ***Figs. S1K-N***. The $\Delta\varphi = 2\pi$ and 3π states relax, with the compressed boundaries of the *b* and *t* structures of the 2π-twist state expanding into the formerly uniform interior (***Figs. S1M,N,D,E***). The field-stabilized *f+* state relaxes to a linear $\Delta\varphi = \pi$ twist (magenta arrow), which, like the *f-* , is extremely dilated relative to the *initial* $\Delta\varphi = 3\pi$ state, but, unlike the *f-*, can increase the twist by changing its surface states, reorienting $\varphi(0)$ and $\varphi(d)$ from their metastable minima back to the preferred polar minima, as sketched in ***Fig. S1L***. One such surface transition generates a 2π–twist state. If *E* is reduced slowly, this process is observed as the motion of domain walls that expand the areas of neighboring 2π-twist states. However if *E* is reduced more quickly (in just a few seconds), a striking instability appears that produces the modulated textures shown in ***Figs. S1A,K,L***. This modulation is possible because the surface reorientations of π can take place on either the top or the bottom surface, giving RH 2π-twist states of diametrically opposing $\boldsymbol{P}(x)$ (***Fig. S1L***). These form a spatially periodic pattern of field-free 2π-twist states, where in each half-period there is one preferred and one metastable surface orientation, alternating between top and bottom between half-periods. The origin of this instability is not clear, but spontaneous periodicity is not uncommon in viscous dynamic LC systems due to the coupling of flow and reorientation in response to conditions of strong driving [4,5].

Once formed upon reducing *E*, these modulated areas can return to the *initial* state at $E \sim 0$ by a process in which the modulation stripes appear to split apart into an array of distinct lines separated by areas which have reverted to configurations with the surfaces aligned along the preferred polar minima, *i.e.*, to the *initial* $\Delta\varphi = 3\pi$ state, resulting in textures of homogeneous *i* areas and irregular remnant lines, as in ***Figs. S1A,O***. These lines are the N_F* analog of oily-streak defects in an N* texture, but, as is the case for all of the N_F phase textures, have $\boldsymbol{n}(\boldsymbol{r})$ and $\boldsymbol{P}(\boldsymbol{r})$ in the *xy*-plane. The structure of these remnant lines at $E = 0$, sketched in ***Fig. S1P***, reflects various mixes of 2π metastable states with one polar, non-preferred surface orientation, or the 3π *reverse* state (*r*) with both surfaces metastable. The *i* state interspersed with these defect lines is the final condition following a positive-*E* cycle starting and ending at zero. Applying a *negative E* field to this modulated starting state splits the defect lines into two walls, with their internal 2πT areas appearing in between. For $E < 0$, the 2πT areas immediately transform into the *f-* state via a surface transition to the favored orientation at the bottom of the cell that relieves the twist there, as illustrated in ***Fig. S1Q***. In the absence of defect lines, the *f-* state can also be reached from the *i* state via the formation and disappearance of a 2π disclination sheet in the cell interior (***Fig. S1Q***), as discussed previously. The $E \sim 3$V/mm range of the field required to ob-

tain the *f* states enables an estimate of the energy difference between the preferred and non-preferred polar surface orientations, by taking a maximum to be $w_P = PE\xi_E = \sqrt{(PEK)} = \sim 3\text{x}10^{-3}$ J/m^2. By comparison, the typical quadrupolar wells of rubbed polyimide films are in the range 10^{-4} J/m^2 < w_Q < 10^{-2} J/m^2.

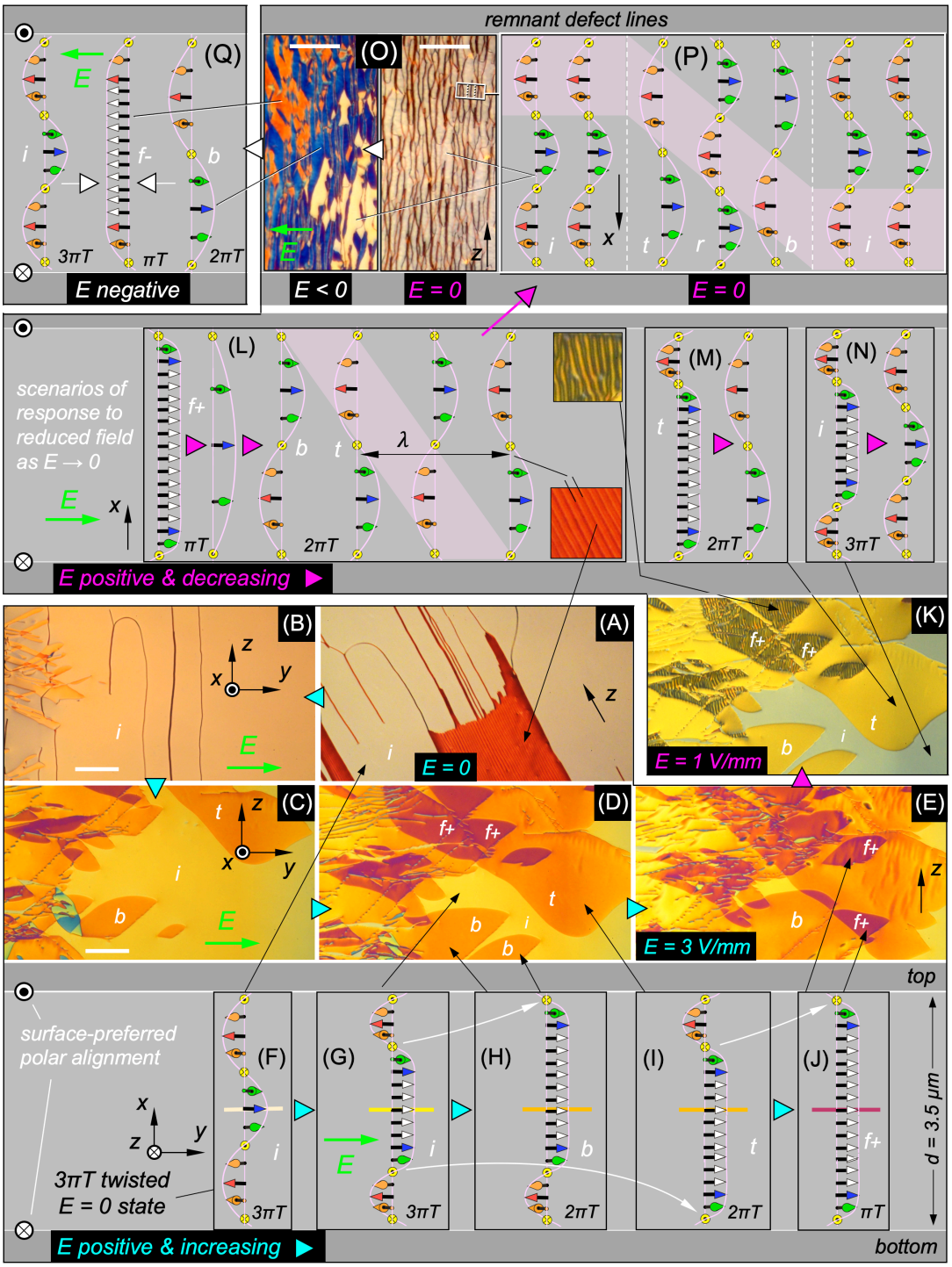

Figure S1: Electric field-induced helix unwinding of the N_F* phase of a chiral RM734/CB15* mixture in a d = 3.5 μm thick *ANTIPOLAR* cell. The white dots/crosses on the left of the gray panels indicate the in-plane polar orientation preference of the surfaces, corresponding to the gray/white arrows in ***Fig. 1***. The observed helical structures are all right handed. The empty cell structure with the field applied is chiral, with a handedness depending on the sign of the field. The cyan, magenta, and white triangles indicate the direction of increasing positive, decreasing positive, and increasing negative field, respectively. (***A-E***) DTLM textures with increasing positive E in the range $0 < E < 3$ V/mm. (***F-J***) Sketches of the local 1D profile of $\boldsymbol{P}(x)$ in the *initial* (*i*), *bottom* (*b*)/*top* (*t*), and *final* (*f+*) states, with ***P*** becoming more uniform as the field is increased. The curved white arrows in this panel indicate surface reorientation transitions, where π twist in the interior of the cell are eliminated by surface reorientation from a stable to a metastable state. The *initial* state (*F*) is a 3π twist with a pitch $p \sim 2.3$ μm. Applied field expands the stable region in the middle of the cell (*G*) and then induces a transition to the *b* and *t* states, which have field-confined π-twists near the cell bottom (*H*) and top (*I*), respectively. Further increase of the field induces a transition to the *f+* state, which has a field-confined π/2 twist on each surface, shown in (*E*). (***K***) Upon reducing the applied field, within a few seconds the *b*, *t* and *f+* domains relax and their boundaries retract to their original locations in (*D*). The *f+* domains exhibit a dramatic instability, breaking up into stripes, remnants of which are also shown in (*A*). (***L***) Schematic drawing of the *f+* domain instability following a reduction in the applied field. The initial *f+* relaxation is to a state of uniform π twist with a pitch three times that of the *i* state and a metastable polar surface orientation on both surfaces. This dilated state relaxes in turn by flipping the orientation at one surface by π, to generate a 2π-twist state. A periodic instability occurs along the *y* direction when such flips occur alternately on the top and bottom surfaces, generating a metastable array of 2π-twist states differing in average orientation by π. (***M,N***) Continuous relaxation of the field-distorted *t* and *i* states when $E \rightarrow 0$. The pink shaded areas in (*P*) and (*L*) highlight regions of common orientation. (***O,P***) The system relaxes further from the 2π-twist states to the homogeneous 3π–twist starting condition, *i*, by relaxation of the remaining metastable surface orientations. A splitting of the periodic array in (*L*) occurs, with the surface-preferred 3π-twist state appearing between remnant, oily-streak-like defect lines. These lines are single- or few-period runs of the original surface-metastable 2π or reverse 3π-twist (*r)* state, as shown in (***P***). Application of a weak negative field further splits the defect lines into two walls, with the interior metastable 2π states appearing in between. These immediately transform into the *f-* state. (***Q***) Since the handedness of the empty cell/field structure changes with the sign of field while that of the N_F* phase is fixed by the dopant, a negative E must produce a completely different sequence of states. The transformation from *i* to *f-* is achieved either by way of a 2π disclination sheet in the cell center, with fixed surfaces, or from a 2π state via the remnant defect lines of ***Figs. S1 O,P***. The *f-* is the lowest energy field-on state, because the surfaces are both at their preferred orientations. Scale bars: 100 μm.

SECTION 2 – Π-TWIST DOMAINS IN THE N_F AND N PHASES

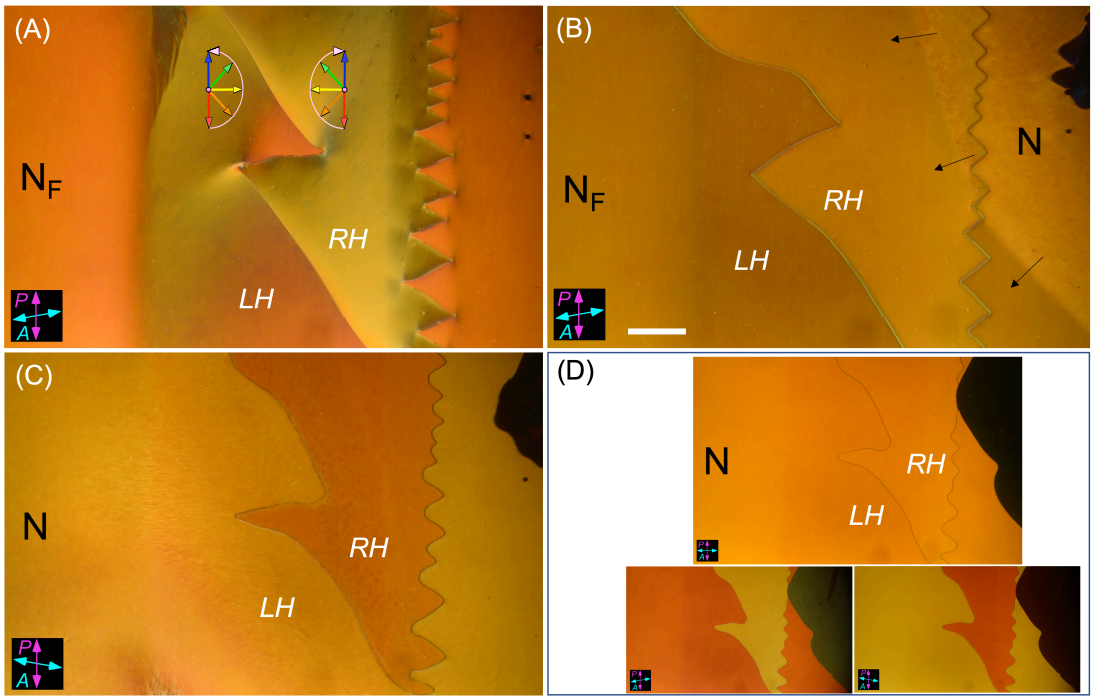

Figure S2: Π-twist domains in a d = 3.5 μm *ANTIPOLAR* cell, showing: (***i***) that such domains in the N_F phase persist into the N phase upon heating through the N-N_F transition; and (***ii***) twisted states in the N_F phase are distorted by in-plane electric fields produced by polarization space charge. (***A***) At T = 125°C the 2πT wall has its characteristic zig-zag shape. Schematics show the π-twist structures. Polarization reversal at the wall in the cell center (yellow arrows) deposits polarization charge at the wall. If unscreened, the resulting in-plane electric field produces the continuous reorientation and color variation, with $\varphi(0) = 0$, $\varphi(d) = \pi$, but an (y,z)-dependent nonlinear field-induced variation in between. The zig-zag structure minimizes and separates the lengths of 2πT wall that run vertically in these images, as this is the orientation has the maximum space charge deposited on the wall. (***B***) Upon heating to the N-N_F transition temperature at T = 133 °C the N-N_F phase front sweeps across the sample (black arrows). Additionally, the zigs and zags in the 2πT wall become less exaggerated, both in the N_F phase and more so in the N phase, as ***P*** decreases and then disappears. (***C,D***) 2πT wall in the N phase, held in by the RP surface energy W_Q. The line tension (excess energy per unit length) of the 2πT wall causes the undulations to straighten out (*C* to *D*). The mirror reflective twist structures give symmetric optical changes for mirror reflective analyzer rotations. (***D***) The π-twist states in the nematic have uniform coloring indicating the field-free linear variation of $\varphi(x)$. The π-twist states in the nematic are metastable. The black domain growing in on the right is the uniform (U) nematic state, which, in absence of the polar alignment energy W_P, minimizes both W_Q and the bulk Frank twist elastic energy. Scale bar: 200 μm.

SI REFERENCES

1 P. Oswald, L. Jørgensen & A. Żywociński, Lehmann rotatory power: a new concept in cholesteric liquid crystals. *Liquid Crystals* ***38***, 601-613 (2020). DOI: 10.1080/02678292.2011.560291.

2 I.I. Smalyukh, Y. Lansac, N.A. Clark, R.P. Trivedi, Three-dimensional structure and multistable optical switching of triple-twisted particle-like excitations in anisotropic fluids. *Nature Materials* ***9***, 139-145 (2009). DOI: 10.1038/NMAT2592

3 M. Schubert, B. Rheinlander C. Cramer, H. Schmiedel, J.A. Woollam, C.M. Herzinger, B. Johs, Generalized transmission ellipsometry for twisted biaxial dielectric media: application to chiral liquid crystals. *J. Opt. Soc. Am. A* ***13***, 1930-1940 (1996). DOI: 10.1364/JOSAA.13.001930

4 E. Guyon, R.B. Meyer, J. Salan, Domain structure in the nematic Freedericksz transition. *Mol. Cryst. Liq. Cryst.* ***54***, 261-2713 (1979). DOI: 10.1080/00268947908084859

5 A.J. Hurd, S. Fraden, F. Lonberg, R. B. Meyer, Field-induced transient periodic structures in nematic liquid crystals :the splay Frederiks transition. *J. de Phys*. ***46***, 904-917 (1985). DOI: 10.1051/jphys:01985004606090500